Hydration Dynamics in a Partially Denatured Ensemble of the Globular Protein Human α-Lactalbumin Investigated with Molecular Dynamics Simulations

Neelanjana Sengupta, Simon Jaud, and Douglas J. Tobias
Department of Chemistry, University of California, Irvine, California

ABSTRACT Atomistic molecular dynamics simulations are used to probe changes in the nature and subnanosecond dynamical behavior of solvation waters that accompany partial denaturation of the globular protein, human α-lactalbumin. A simulated ensemble of subcompact conformers, similar to the molten globule state of human α-lactalbumin, demonstrates a marginal increase in the amount of surface solvation relative to the native state. This increase is accompanied by subtle but distinct enhancement in surface water dynamics, less favorable protein-water interactions, and a marginal decrease in the anomalous behavior of solvation water dynamics. The extent of solvent influx is not proportional to the increased surface area, and the partially denatured conformers are less uniformly solvated compared to their native counterpart. The observed solvation in partially denatured conformers is lesser in extent compared to earlier experimental estimates in molten globule states, and is consistent with more recent descriptions based on nuclear magnetic relaxation dispersion studies.

INTRODUCTION

Solvation plays a vital role in protein structure, dynamics, and function. The wide variety of studies that have elicited the dependence of such properties on protein solvation include light scattering and fluorescence experiments (1–5), small-angle x-ray and neutron scattering spectroscopy (6–12), nuclear spin echo (13,14), solid-state NMR (15), nuclear magnetic relaxation dispersion (16–20), Fourier transform infrared (FTIR) measurements (21), and terahertz spectroscopy (22–25). In addition, molecular dynamics simulations have been used extensively to characterize the dynamics of protein solvation (26–30) and its association with protein conformation, function, and dynamics (10,11,31–35). It is important to note that solvent effects are understood to play a fundamental role in protein folding and unfolding (36–40). For example, a simulation study of the SH3 protein identified the existence of an ensemble of ''near-native'' structures, the transition to the native state being facilitated by expulsion of water molecules from the core of the protein (40). A coarse-grained simulation of protein-solvent systems has been used to suggest that loss in conformational entropy in the folding protein is compensated by gain in translational entropy of solvent particles (41). It has been seen that protein folding and unfolding kinetics can be modulated by solvent viscosity (42,43).

It is now well accepted that most nascent protein polymers encounter at least a few metastable states en route to the natively folded functional form, and developing a knowledge of the intermediates is vital for developing an understanding of the folding process (44,45). The transition pathways connecting the metastable states may not be unique, and the folding ensemble is comprised of a large number of energetically equivalent substates. The loss in conformational entropy as the protein progresses toward the folded form implies that the ensemble ''size'', or heterogeneity, should decrease along the folding pathway. In view of the fundamental relationship between protein solvation and dynamics, it is important to understand the dynamical and energetic changes in the protein solvating layer that accompany the folding or unfolding process (38,39). Recent studies with fluorescent probes attached to the protein surfaces and dynamic light-scattering experiments have elucidated differences in solvation times between the fully denatured, ''premolten'' globule, molten globule, and native states (3,4). Molecular dynamics simulations have been used to point out clear differences in the secondary structure dependence of solvation dynamics between the native and a hypothetical molten globule state of the protein HP-36 (46). Simulations have also been used to correlate partial unfolding of specific secondary structure elements with mobility of the solvation layer and the protein-water hydrogen bonding kinetics (47). Site-specific mutations and solvation correlation functions constructed from femtosecond-resolved fluorescence transients show site-dependent enhancement of water dynamics in the molten globule state compared to the native state of myoglobin (5).

Despite recent developments, there remains a lack of understanding of the changes in some general, but presumably important, aspects of protein solvation, such as the extent, anomalous behavior, and energetic interactions as a protein proceeds along its folding pathway. In this study, we attempt to understand the dynamical changes in protein solvation accompanying partial denaturation of the globular protein human α-lactalbumin (HαLA), which occur on timescales up to a few hundred picoseconds. We use molecular dynamics

Submitted May 2, 2008, and accepted for publication July 28, 2008.

Address reprint requests to Douglas J. Tobias, Dept. of Chemistry, University of California, Irvine, CA 92697. E-mail: dtobias@uci.edu.

Editor: Arthur G. Palmer 3rd.

0006-3495/08/12/5257/11 $2.00

doi: 10.1529/biophysj.108.136531

(MD) simulations to create an ''ensemble'' of partially denatured conformers that are conformationally stable over those timescales. In this respect, and in the extent of their loss of compactness relative to the native (N) state, the members of our ensemble resemble the subcompact molten globule (MG) state of HαLA. The metastable MG states are thought to be the equilibrium analogs of early folding intermediates in globular proteins (44,48–50), and it has even been recognized that they have pathologically important roles (51,52). Compared with the native state, we find consistent changes in the dynamical behavior of the solvation waters in our partially denatured ensemble. These changes are such that the well-known slowdown of protein surface waters relative to bulk (11,16,17,27,28,30,53–55) is decreased or, in other words, there is a shift toward bulklike behavior. This shift is subtle but distinct, and is observed for both translational and rotational dynamics of the solvating waters, and found to be widely distributed over the ensemble. Increased dynamics is also accompanied by marginally greater solvation in almost all ensemble members. The average increase in the solvation number (N_s) is, however, much less than the quantities reported in earlier experimental studies of MG states (13,56,57). We have used the dynamical second-rank rotational correlation function calculated from our simulations in combination with the surface solvation number to obtain the NMRD hydration parameter $N_s\rho_s$ (18). The average value of this quantity for the partially denatured ensemble is very close to the value for the native-state simulation. This finding is in agreement with the observed constancy of $N_s\rho_s$, within error limits, during the N$\rightarrow$MG transition for a variety of proteins (18).

When comparing our results to experimental data, it is important to keep in mind the disparity in conformational sampling: experiments reporting the average behavior of 10^{15}–10^{18} molecules often fail to describe the behavior of an individual species, whereas the longest atomistic MD simulations will not encompass all conformers present in an experimental sample (38). Extensive sampling is required to characterize properties of metastable intermediates that exchange on long timescales and form ensembles with a high degree of heterogeneity. The consistent changes observed in our ensemble of partially denatured conformers, whose level of compactness is similar to the MG state of HαLA, ought to be suggestive of phenomena occurring in actual MG samples. The quantities measured experimentally are likely to be closer to the ''ensemble average'' than to quantities obtained from any single simulation. A previously reported protocol for creating large ensembles of conformers structurally similar to the experimental MG state of HαLA involved denaturation by application of biasing forces in a continuum solvent (58). In this study, we focus on characterizing the changes in dynamical behavior of the solvation molecules brought about by partial protein denaturation in implicit solvent, by creating a modest-sized ensemble that is subsequently investigated using simulations in explicit solvent. A similar thermal denaturation protocol has been implemented in a study of solvation in the native state and a representative MG conformer of another globular protein (46). Our conformers, with radii of gyration stable over the timescale of interest, may reasonably be assumed to have solvation water dynamical properties akin to those of MG conformers with a similar loss in compaction.

METHODS

Simulation protocol

The 1.7-Å resolution x-ray crystal structure of HαLA, obtained from the Protein Data Bank, entry 1A4V (59), was the starting point from which partially denatured conformers were created (59). For computational efficiency, a thermal unfolding process was simulated with the native protein structure placed in an implicit solvent environment. Implicit solvent models represent the solvent as a dielectric continuum, in contrast to including the solvent molecules explicitly. The generalized Born solvent area (GB/SA) implicit solvent model was used (60), and the simulation was carried out with the Maestro simulation program (Schrodinger, Portland, OR). A cutoff of 20 Å was set for electrostatic calculations, 8 Å for van der Waals interactions, and 4 Å for hydrogen bonding, and the dielectric constant was set to 78. Initially, the protein-solvent system was heated over a period of 1 ns, with the temperature increased gradually from 50 to 300 K. This did not cause any significant unfolding in the structure, and the radius of gyration (R_g) of the system remained close to the native value of 14.35 Å (59). The temperature was then set to 400 K, and the system responded with a jump in the R_g. At this temperature, the maximum R_g of 18.45 Å was reached in 50 ps, soon after which the system contracted, with R_g values settling in the vicinity of 16 Å. The unfolding behavior of the protein in implicit solvent for a period of 2 ns is shown in Fig. 1. There is a slow conformational change between 0.5 and 2 ns, as seen from the gradual rise in R_g during that time span. However, the conformations correspond to the experimentally measured R_g range of 16–19 Å (1).

Ten roughly equispaced conformational snapshots from the simulation trajectory were subjected to independent simulation runs of 200 ps in implicit solvent. The conformations at the start and end of these individual simulations were then selected to represent 20 putative members of a partially denatured ensemble. This method ensures the conformational heterogeneity of the ensemble while maintaining the experimentally determined extent of denaturation. To model conformers similar to the low-pH ''A'' state of the HαLA molten globule (61), the glutamate, aspartate, and histidine side chains and the C-terminus were protonated, the Ca^{2+} ion was removed, and 16 Cl^- counterions were added. Fifteen of these partially denatured conformers (randomly selected) were transferred to a preequilibrated box of water measuring ~57 Å on each side. The R_g of the selected systems at this

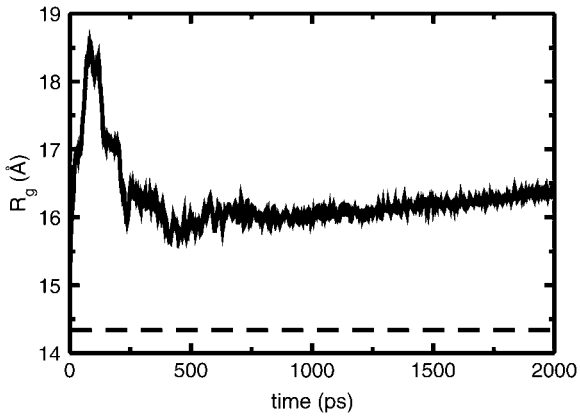

FIGURE 1 The unfolding behavior of the compact native HαLA in implicit solvent at 400 K.

stage have been listed in Table 1. The SPC/E water model (62) was employed, as it has been shown to accurately describe dynamical aspects of protein hydration (53). From that point, the explicitly solvated systems were simulated using the NAMD simulation program (63), with the CHARMM22 all-atom force field for the protein (64). After 50 ps of conjugate gradient energy minimization, each solvated protein system was individually simulated at a pressure of 1 atm and a temperature of 296 K. Constant temperature was maintained using Langevin dynamics with a collision frequency of 1 ps^{-1}. The Nosé-Hoover Langevin piston algorithm (65,66), as implemented in the NAMD package, was used to maintain constant pressure. The lengths of bonds involving hydrogen atoms were held fixed with the SHAKE algorithm (67). A simulation time step of 1 fs and periodic boundary conditions were employed. Electrostatic interactions were calculated with particle mesh Ewald (68). The real-space electrostatic and van der Waals cutoff distances were set at 11 Å, with smooth truncation starting at 10 Å. The R_g of each system took between 3.5 and 6.5 ns to settle within the 16–19 Å range, after which the systems were equilibrated at constant volume for 500 ps. The dynamical correlation functions investigated in this study largely decay within the first 100 ps. Thus, our production runs consisted of 400 ps of constant-energy MD, with coordinates saved every 0.1 ps. For comparison, a simulation of the explicitly solvated native state of HαLA was performed within the same protocol. The R_g of the native and the 15 partially denatured states during the production runs remained stable, as seen in Fig. 2. The backbone root mean-squared deviations (RMSDs) of the conformers relative to the native crystal structure are found to be stable during the production runs (data not shown). The mean values of the R_g and the backbone C^α RMSD are given in Table 1. Fig. 3 shows snapshots of the native and denatured states at the beginning of the production runs created with the Visual Molecular Dynamics program (69).

Analysis methodology

Solvent residence times and mean-squared displacement

The residence time correlation function from which the average survival time is calculated, is obtained from the equispaced production run configurations as

$$R_A(t) = \frac{1}{N(t)} \sum_{t_0} \sum_{j=1}^{N_w} p_{A,j}(t_0, t_0 + t). \quad (1)$$

TABLE 1 Radii of gyration and RMSDs of native (N) and 15 partially denatured protein systems

System	R_g (Å)		RMSD (Å)
	At denaturation	Production run	Production run
N	—	14.31	1.12
1	17.34	16.24	5.80
2	16.50	15.93	4.31
3	17.20	16.40	5.60
4	15.90	15.73	4.80
5	17.90	15.51	3.43
6	16.91	16.10	4.74
7	16.10	15.40	3.74
8	16.30	15.50	3.90
9	19.60	15.70	6.14
10	19.10	17.80	7.60
11	17.04	15.91	4.30
12	16.50	15.90	4.00
13	16.70	15.31	3.40
14	17.70	17.40	6.80
15	18.50	15.22	2.84

For radius of gyration (R_g), values given are before equilibration in explicit solvent and averaged over constant-energy production runs. The RMSD of the backbone C^α atom is given with respect to the native crystal structure.

Here, the binary function $p_{A,j}(t_0,t_0 + t)$ assumes a value of 1 if the jth water molecule remains within the solvation layer of site A continuously for time t, starting from an arbitrary time origin t_0, and 0 otherwise. N_w is the total number of water molecules in the system. The correlation function is calculated with a moving time origin t_0, and $N(t)$ is the number of segments corresponding to each time span t. Each of the 123 amino acid residues of HαLA has been treated as a ''solvation site''. The mean residence times are obtained from exponential fits of the normalized correlation functions, $R_A(t)/R_A(0)$. The histograms of the mean residence times for each system are used to obtain the arithmetic minimum, maximum, and average residence time. The average residence time obtained in this manner can be compared to the mean residence time of waters solvating the entire protein system, calculated from the function $R_P(t)$, which has the same functional form as $R_A(t)$ but is constructed as an average over all sites. We fit the normalized residence correlation function obtained for the entire protein to the stretched exponential, known as the Kohlrausch-Williams-Watts (KWW) function,

$$\frac{R_P(t)}{R_P(0)} = e^{-(t/\tau)^\lambda}. \quad (2)$$

The integral of the stretched exponential function gives the mean solvent residence time around the protein,

$$\langle \tau_P \rangle = \frac{\tau}{\lambda} \Gamma\left(\frac{1}{\lambda}\right). \quad (3)$$

The diffusion of water molecules in the protein solvation layer is known to be described by non-Brownian kinetics (27). In this ''dispersive diffusion'' regime, the mean-squared displacement (MSD) of the water oxygen atoms within the solvation layer is fitted to the power-law form

$$\langle r^2(t) \rangle \propto t^\alpha. \quad (4)$$

The coefficient α, compared to the value obtained for bulk water, gives a direct measure of the anomalous nature of surface solvation.

Rotational dynamics and ^{17}O NMRD parameters

We highlight the salient features of quadrupolar spin relaxation theory as required by this study. For greater appreciation of the theoretical framework and applications of the nuclear magnetic relaxation dispersion (NMRD) technique, the reader is referred to a comprehensive series of articles by Halle et al. (16,17,70–73). From the theoretical foundations of quadrupolar spin relaxation theory, the ^{17}O NMRD longitudinal relaxation rate profile depends on the resonance frequency, ω_0, as follows (17,70):

$$R_1(\omega_0) = R_{bulk} + \alpha + \beta \tau_c F_1(\omega_0 \tau_\beta). \quad (5)$$

The term $\beta \tau_c F_1(\omega_0 \tau_\beta)$ is the frequency-dependent dispersion step describing the slow rotation of the protein molecule and its associated integral waters, and R_{bulk} is the frequency-independent relaxation rate of bulk water. Here, α describes the relaxation parameters of water molecules near the protein surface, which can be expressed as

$$\alpha = \left(\frac{N_s}{N_T}\right)(\langle R_s \rangle - R_{bulk}), \quad (6)$$

where N_s and N_T are, respectively, the number of surface water molecules and the total number of water molecules, and $\langle R_s \rangle$ is the average surface relaxation rate. The quantity obtained from the experimental relaxation profiles is

$$N_s \rho_s = \frac{\alpha N_T}{R_{bulk}} = N_s \left(\frac{\langle R_s \rangle}{R_{bulk}} - 1\right). \quad (7)$$

Since the ^{17}O quadrupolar coupling constant is expected to be the same for water molecules next to the protein surface and in bulk water (16), $\langle R_s \rangle / R_{bulk}$

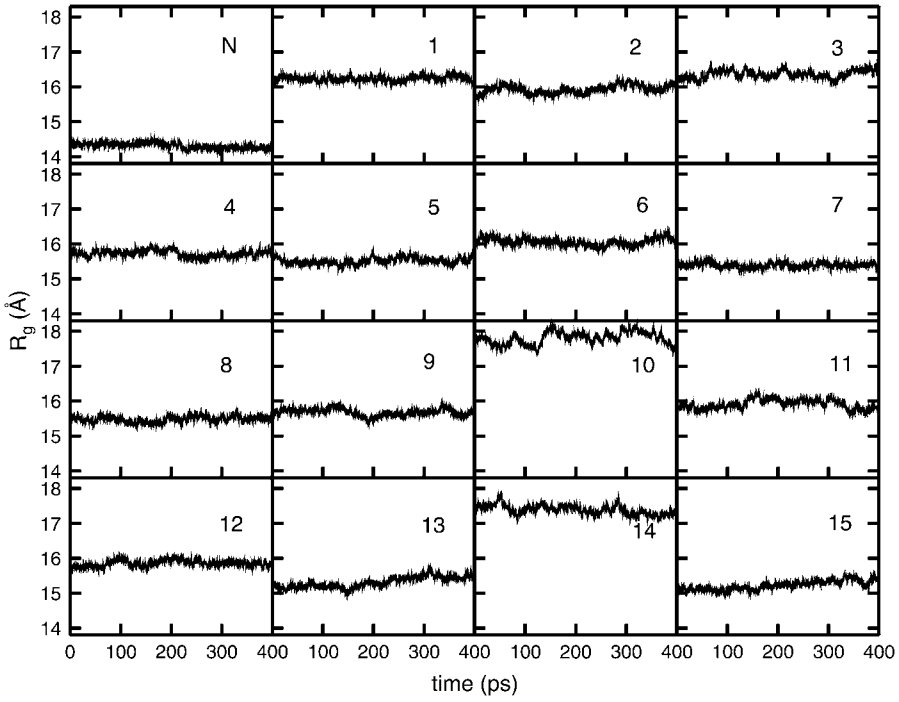

FIGURE 2 Radii of gyration (R_g) of the native (N) and 15 partially denatured protein conformers during the equilibrated, constant energy production runs.

may be interpreted as the ratio ($\langle\tau_s\rangle/\tau_{bulk}$) of the average second-rank rotational correlation times. Thus,

$$N_s\rho_s \approx N_s\left(\frac{\langle\tau_s\rangle}{\tau_{bulk}} - 1\right). \quad (8)$$

Estimates of rotational relaxation times of bulk and surface waters are computed from the simulations via time correlations of the second Legendre polynomial (the second-rank spin correlation function),

$$P_2(t) = \left\langle \frac{3\cos\theta(t)^2 - 1}{2} \right\rangle, \quad (9)$$

where $\theta(t)$ is the rotation angle of a molecule fixed unit vector in time t. We have chosen the dipole moment vector of the water molecule for this calculation and we have found that the OH vector gives essentially identical results. It is known that $P_2(t)$ does not have a simple exponential decay, but can be fitted to the KWW function (28,54). The region beyond the initial transient decay is therefore fitted to the form

$$P_2(t) = e^{-(t/\tau)\beta}, \quad (10)$$

and the mean relaxation time is computed using

$$\langle\tau\rangle = \frac{\tau}{\beta}\Gamma\left(\frac{1}{\beta}\right). \quad (11)$$

RESULTS

Definition of the solvation layer from native state results

It has been shown that accuracy of NMRD results obtained from simulation studies has a dependence on the definition of the solvation layer (28). In Table 2, we report for the native simulation the average solvation number, N_s, the rotational

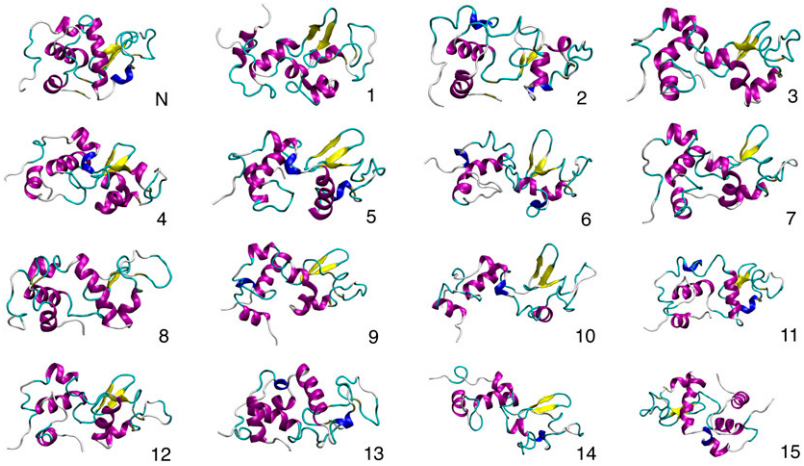

FIGURE 3 Snapshots of the native (N) and 15 partially denatured conformers at the beginning of the constant energy simulation runs. Helices are in purple and blue, β-sheets in yellow; coils in cyan; and turns in white. Most of the native secondary structure is preserved in the denatured conformers.

TABLE 2 Native-state solvation parameters for different definitions of the hydration layer

Solvation layer thickness (Å)	N_s	$\langle\tau_s\rangle$ (ps)	ρ_s	$N_s\rho_s$ (10^3)	SASA/N_s (Å^2)
3.75	425.72	11.93	5.34	2.270	17.12
4.0	503.85	9.54	4.07	2.048	14.57
4.25	575.54	8.06	3.28	1.886	12.54
4.50	642.27	6.99	2.71	1.741	11.24
4.75	704.23	6.25	2.32	1.631	10.25

parameters $\langle\tau_s\rangle$ and ρ_s, $N_s\rho_s$, and the solvent-accessible surface area per hydration water at varying thicknesses of the solvation layer, defined as the distance between a water O atom and any protein heavy atom. The experimental value of $N_s\rho_s$ is reproduced satisfactorily between 3.75 and 4.75 Å. At 4.0 Å, the solvation number and the retardation factor ρ_s are similar to reported experimental estimates (18). At this thickness, the protein solvent-accessible surface area (SASA) per surface water molecule, calculated by running a probe of 1.8 Å on the protein surface and dividing the total area covered by the number of water molecules within the defined solvation layer, is close to the value of 15 Å^2, the value considered in estimating N_s from NMRD data (18). In this study, we chose the thickness of the solvation layer to be 4.0 Å, i.e., solvation properties in the native and partially denatured states are compared based on water molecules that reside within this distance of the protein surface. This definition is consistent with the radial solvent density profiles around protein heavy atoms obtained from x-ray diffraction data (74). A similar dimension of the first hydration shell has been deduced from small-angle x-ray and neutron scattering data (7,75).

Solvent residence times in native and subcompact states

In Fig. 4, we show the residence time correlation function of waters solvating the entire protein within the solvation layer. A shift toward shorter relaxation times occurs consistently for each of the denatured states. The overall shift is modest, with a 31.2% decrease in the mean residence time calculated from $R_P(t)$ relative to the N state, when averaged over all of the ensemble members. The shift is more pronounced within the first few tens of picoseconds (Fig. 4, *inset*), which indicates weaker association of the protein with the surface waters. We note that the fitting parameter λ does not change significantly between the native and partially denatured conformers, and the decrease in the mean residence time is mainly due to the change in parameter τ. The residence-time data is summarized in Table 3. The shift toward shorter residence times is also evident when the histograms of the individual residence times (calculated from the time correlation functions at each amino acid residue, as described in Methods are considered (Fig. 5). Based on the data in Fig. 5, the shortest residence times, averaged over the ensemble, decrease by 84% relative to the native value of 2.6 ps, whereas the longest times decrease by 70.7% relative to the native value of 240.7 ps. This supports the idea that the larger contribution to the overall shift is due to water molecules that reside on the protein surface for a few tens of picoseconds, as seen from the inset in Fig. 4. For the entire ensemble, the average residence time from the histograms decreases by 37.1% relative to the corresponding native state value. The mean residence time from $R_P(t)$ and the average residence times from the histograms agree fairly well. The small differences in the two quantities can be attributed to overlap in the water molecules in the solvation layer definition of neighboring amino acid residues.

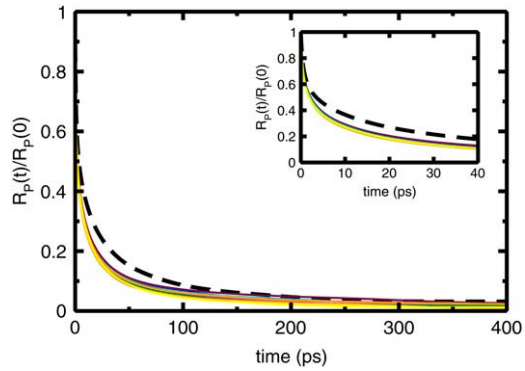

FIGURE 4 Normalized residence-time correlation functions of waters solvating the entire protein molecule, for the native state (*dashed line*) and the 15 partially denatured simulations (*colored lines*). (*Inset*) Residence-time correlation functions, shown for the native and partially denatured conformers, rapidly decay on a timescale of tens of picoseconds.

Translational and rotational dynamics

The mean-squared displacement of the solvation waters in the native state and the partially denatured simulations, as

TABLE 3 Solvent residence times

	Histogram data (ps)			Data from time correlation function	
System	Minimum	Maximum	Average	λ	$\langle\tau_P\rangle$ (ps)
N	2.60	240.70	22.60	0.45	25.90
1	0.31	239.74	14.60	0.38	16.10
2	0.60	44.70	13.80	0.37	18.23
3	0.40	41.80	13.80	0.38	20.44
4	0.10	64.01	14.24	0.40	15.83
5	0.50	47.71	15.34	0.39	16.21
6	0.50	73.60	14.23	0.37	19.20
7	0.50	109.20	14.34	0.37	18.40
8	0.10	43.40	14.62	0.37	19.80
9	0.70	53.10	16.13	0.38	18.20
10	0.60	38.03	14.50	0.38	16.30
11	0.30	46.41	12.70	0.38	16.23
12	0.50	124.20	13.52	0.36	22.23
13	0.20	39.72	14.01	0.39	17.10
14	0.62	37.63	15.13	0.38	17.05
15	0.31	53.30	12.41	0.39	16.10

Data were obtained from histograms of average times at individual residues, and from a fit of the survival-time correlation function of the entire solvation level to a stretched exponential.

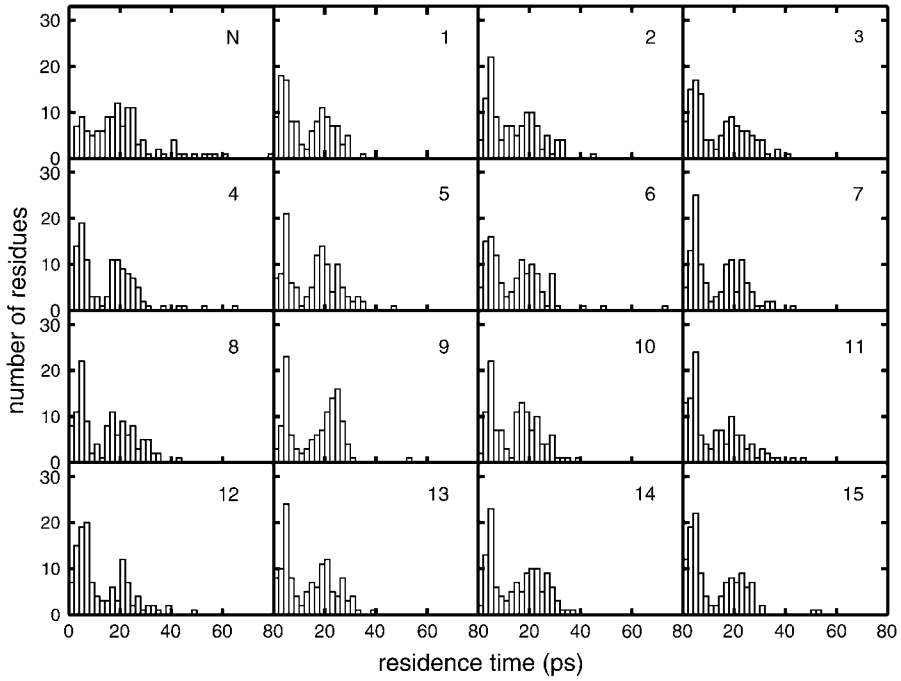

FIGURE 5 Histograms of average residence times obtained at each amino acid residue from exponential fits of individual residence-time correlation functions for the native (N) and 15 partially denatured conformers. There is a distinguishable shift toward shorter residence times in the partially denatured conformers.

well as that obtained from a simulation of bulk SPC/E water are shown in Fig. 6. Our constant-energy simulation of bulk water, equilibrated at 296 K and 1 atm pressure, yields a diffusion coefficient of 2.5×10^{-5} cm^2/s compared to the experimental value of 2.4×10^{-5} cm^2/s at 300 K (62). It is obvious from the figure that the solvent diffusion on the protein surface is significantly slower than the diffusion in bulk water. This is consistent with observations reported in previous studies with other proteins (27,28,30,53,55). A value of $\alpha < 1$ is a signature of anomalous diffusion of water molecules close to the protein surface. In Table 4, we report the parameter α obtained from the power-law fit of the mean-squared displacements in the diffusive regime. For the native-state simulation, $\alpha = 0.74$ is in good agreement with that obtained in the 4-Å solvation layer of copper plastocyanin (27). Although the α-value is significantly less than the bulk value for all protein systems, it is consistently larger for each member of the partially denatured ensemble compared to the native state. Thus, the transition from the N to the subcompact states is characterized by reduced anomaly in the diffusive behavior in hydration waters, with a shift toward bulk-like behavior.

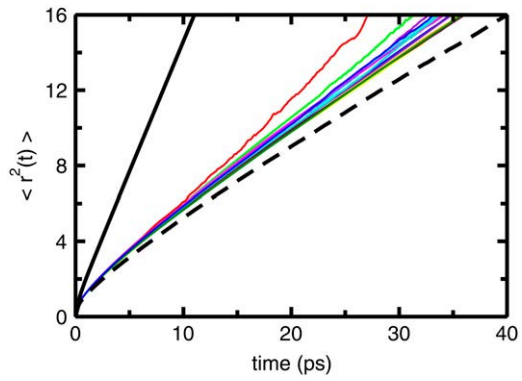

FIGURE 6 Mean-squared displacement of water molecules within the hydration layer of the native (*dashed line*) and 15 partially denatured protein systems (*colored lines*). The solvent displays a decrease in anomalous diffusive behavior in the partially denatured systems. For comparison, the mean-squared displacement of bulk water is also shown (*solid black line*).

TABLE 4 Dynamical data for the protein solvation layers in the native (N) and 15 partially denatured conformers

System	N_s	SASA/N_s (Å^2)	α	β	$\langle\tau_S\rangle$	ρ_s	$N_s\rho_s$ (10^3)
Bulk water	—	—	0.90	0.67	1.88	—	—
N	503.90	14.60	0.74	0.43	9.54	4.07	2.05
1	554.98	16.12	0.79	0.45	7.84	3.16	1.75
2	550.70	15.73	0.77	0.45	8.09	3.29	1.81
3	556.32	15.34	0.79	0.43	8.42	3.47	1.93
4	496.23	17.30	0.77	0.45	7.57	3.02	1.50
5	543.80	15.50	0.77	0.44	8.59	3.56	1.93
6	551.50	16.01	0.77	0.43	9.07	3.81	2.10
7	533.14	14.90	0.78	0.42	8.86	3.70	1.97
8	520.32	15.74	0.79	0.42	9.18	3.87	2.02
9	547.92	15.70	0.79	0.43	8.56	3.54	1.94
10	598.80	15.04	0.84	0.45	7.51	2.99	1.79
11	560.10	15.40	0.79	0.42	9.13	3.84	2.15
12	520.54	16.00	0.77	0.43	9.21	3.90	2.02
13	546.62	15.30	0.78	0.46	7.70	3.09	1.79
14	594.83	15.12	0.80	0.44	8.04	3.27	1.95
15	510.30	16.11	0.79	0.44	7.76	3.12	1.60

The hydration number (N_s) and the SASA/N_s were averaged over the production runs. α-values were obtained from the power-law fit of the mean-squared displacement, and τ_S and β from the stretched exponential fit of the dipolar second-rank relaxation.

Fig. 7 shows the time evolution of the second-rank rotational correlation functions of hydration waters in the native and partially denatured states, as well as for bulk water. Consistent with the decreased residence times and enhanced translational dynamics discussed above, the rotational correlation function decays faster for waters solvating the partially denatured proteins relative to those solvating the native state conformer. In Table 4, we also report the parameters obtained from a fit of $P_2(t)$ to the stretched exponential form after the initial transient decay. The mean rotational time is noticeably shorter for most of the partially denatured conformers. Similar to the behavior of the residence-time correlation functions, the stretching parameter, β, does not change significantly between the native and partially denatured forms, and the decrease in the mean rotational correlation time is mainly due to a change in τ. Considering the entire denatured ensemble, the mean rotational time is found to decrease by 12.3% relative to the native state value.

As described earlier in Methods, the mean rotational time of a protein from $P_2(t)$ can be combined with the corresponding value in bulk to obtain the quantity ρ_s ($\langle\tau_s\rangle/\tau_{bulk} - 1$). The quantity extracted from the high-frequency region of NMRD relaxation profiles is the parameter $N_s\rho_s$. In Table 4, we report the values of $N_s\rho_s$ obtained from our native and partially denatured simulations of HαLA. The native state value of $N_s\rho_s$ (2.05×10^3) is quite close to the quantity measured experimentally ($1.83 \pm 0.16 \times 10^3$) for the homologous bovine α-lactalbumin (BαLA) (18). We mention here that, to our knowledge, no significant difference has previously been found in the measured $N_s\rho_s$ between the native and the partially denatured molten globule state for a variety of conformationally different proteins (18). The $N_s\rho_s$ of our partially denatured ensemble lies in the range ($1.88 \pm 0.18 \times 10^3$), which is very close to the experimental value of ($2.0 \pm 0.2 \times 10^3$) obtained for the MG state of BαLA.

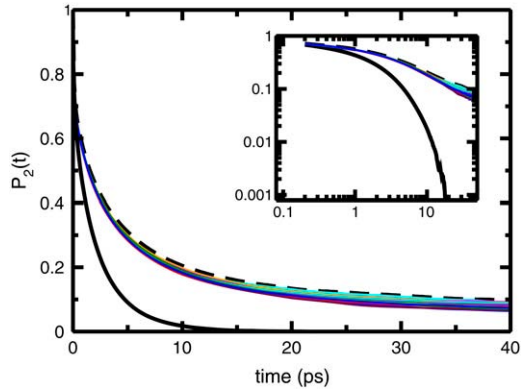

FIGURE 7 Second-rank rotational correlation function for hydration water dipoles in the native (*dashed line*) and partially denatured protein systems (*colored lines*). The decay of the rotational correlation functions in the partially denatured states is characterized by shorter rotational times. The corresponding correlation function for bulk water is also shown (*solid black line*). (*Inset*) Log-log plot of the correlation functions.

DISCUSSION AND CONCLUSIONS

In this report, we have highlighted changes in a few aspects of protein solvation that occur when a globular protein moves from its natively folded to a partially denatured form, or vice versa. We have chosen an ensemble of conformers that are subcompact relative to the native state. As most of the native secondary structural elements are preserved (Fig. 3), and owing to conformational stability in the subnanosecond time regime evidenced by their stable R_g values, which are similar to experimental values, the partially denatured ensemble may be considered a reasonable representation of the MG state of HαLA for the purpose of studying surface hydration dynamics. Based on our results, we can infer that solvent dynamics in such metastable intermediates along the protein folding pathway should be faster compared to the native state. The reduction in the mean residence and mean rotational relaxation times are due to changes in the values of the characteristic times obtained from fits of the correlation functions to stretched exponentials, and the stretching parameter from the fit of these functions to the KWW form is not affected significantly. The native state is also marked by greater anomaly in the diffusion of its solvation waters compared to the denatured ensemble. It should be remarked here that anomalous diffusion of solvation waters is ascribed to topological disorder of the protein surface, or to temporal disorder arising from heterogeneity of the protein energy landscape (30). In this case, the changes in the parameter α obtained from fits of the mean-squared displacement to the power law form, along with the relative insensitivity of the stretched exponential parameters, denote a complexity in the two types of contribution. Although a relative decrease in surface roughness in the partially denatured conformers could lead to less anomaly of the surface waters, the fact that the native and partially unfolded forms occupy different regions of the folding landscape could also play a role. Further studies would be required to fully discern the relative contributions of either factor to the observed phenomenon.

The dynamical differences from the native state, observed consistently for each partially denatured conformer, suggest that the protein-water interactions in the two states may be different. To verify this, we have calculated the total energy of interaction (electrostatic and van der Waals) of every solvation water molecule with the protein, using the NAMDEnergy plugin of the Visual Molecular Dynamics program (69) (Table 5). In Fig. 8, we show histograms of these water-protein interaction energies from equispaced snapshots of the production runs, normalized such that the integrals of the histograms equal N_s in each system. The figures indicate that the interactions are more favorable in the native state compared to the partially denatured states. The native state histogram peaks at -3.5 kcal mol^{-1}, whereas the corresponding value for the denatured ensemble is approximately -2.0 kcal mol^{-1}. The mean protein-solvent interaction energy is -8.23 kcal mol^{-1} for the native state,

TABLE 5 Average protein-solvent interaction energies

System	E (kcal mol^{-1})
N	−8.2
1	−5.7
2	−5.6
3	−5.7
4	−5.5
5	−5.5
6	−5.5
7	−5.8
8	−5.8
9	−5.6
10	−5.3
11	−5.6
12	−5.7
13	−5.5
14	−5.4
15	−5.5
Average (1–15)	−5.6

and −5.60 kcal mol^{-1} for the partially denatured states. Compared to the native conformer, the core region of the partially denatured conformers has greater probability of interaction with solvent water molecules. The large number of hydrophobic side chains lying at the protein core may therefore contribute to an overall decrease in favorability of the aqueous interactions. The small but distinct shift toward less favorable solvent interactions for the denatured ensemble reinforces the role of water in the marginal stabilization of the native state.

In Table 4, we have reported the average number of water molecules (N_s) solvating the protein systems during the production runs. The loss of compaction is accompanied by solvent penetration into the protein interior for all but one of the partially denatured states. The ensemble average of the solvation number represents an 8.3% increase over the native state, which is much less than the increase predicted by earlier studies (56). We also report the SASA/hydration number for every system. The SASA/hydration number shows a consistent increase over the native-state value for each member of the partially denatured ensemble. Thus, the average surface density of water molecules is lower in the partially denatured ensemble compared to the N state. The increase in the SASA/hydration number indicates that the increase in solvation is not proportionate to the extent of exposure of the protein interior, due to the change in the nature of protein-surface interactions. In Fig. 9, we display the water isodensity surfaces within the solvation layer of the native and each partially denatured conformer, averaged over snapshots taken every 2 ps during the production runs. The contour level of the density isosurfaces was chosen to depict regions of high density/probability, which can be considered as water ''binding sites'' on the surface of the protein (76). It is evident from Fig. 9 that the density of water binding sites is higher, and their distribution more uniform, in the N state compared to the partially denatured ensemble. In short, the transition from the native to the partially denatured (MG-like) ensemble appears to be accompanied by a loss of well-defined water binding sites on the surface of the protein.

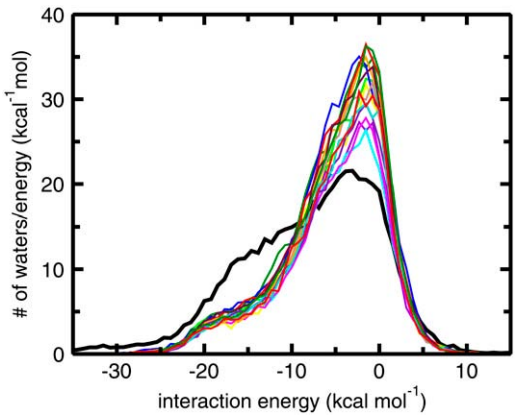

FIGURE 8 Histograms of the energy of interaction of solvent water molecules with the protein for the native state (*solid black line*) and the partially denatured conformers (*colored lines*).

We can draw an important conclusion regarding the extent of surface hydration in MG states from the results of this study. To do so, it is first necessary to point out a few apparent discrepancies that have existed in the understanding of solvent penetration during the N→MG transition. With densitometric studies, as well as sound velocity and absorption studies, it has been seen that for such a transition in HαLA the partial molar volume has a negligible increase, whereas the increase in compressibility is much less than in the melting of macroscopic organic solids. This information, combined with the observation of a 1.42-fold increase in the hydrodynamic (Stokes) radius, has been translated to an influx of 270 water molecules into the interior of the protein during the transition (56). The hydration number of α-lactalbumin has been estimated to be in the vicinity of 500 from the total surface area of the protein crystal structure (18,77), and hence, the calculated data imply an MG surface ~55% more hydrated than the N state. Such a large increase in hydration has also been proposed in ^{1}H NMR and spin diffusion studies of the N→MG transition in the larger carbonic anhydrase B protein (13). The highest water signals in the spin diffusion spectra are found for the MG state, perhaps indicating that the MG state is closely associated with a much larger number of water molecules. Although this study does not quantify solvent penetration, it seems to generally agree with the extensively solvent-penetrated picture of the MG presented earlier based on HαLA (56).

In contrast, NMRD studies have reported that the hydration parameter $N_s\rho_s$ remains nearly constant as a globular protein goes from the N to the MG state (18,78). This phenomenon has been consistently observed for a variety of globular proteins of widely differing size, secondary structure, number of water-binding sites, and, indeed, values of measured $N_s\rho_s$. For the hydration number, N_s, to increase

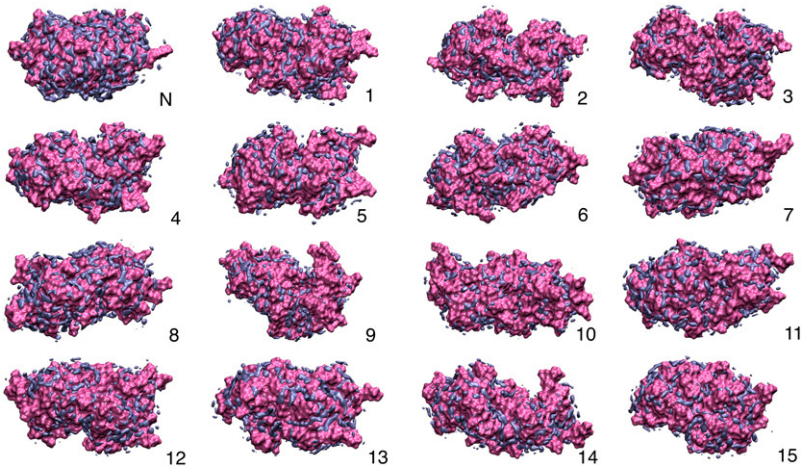

FIGURE 9 Water isodensity surfaces (*light blue*) on the protein surface (*pink*) of the native (N) and 15 partially denatured conformers.

dramatically during the N → MG transition, there would have to be a corresponding decrease in ρ_s to compensate for it; in the case of HαLA, this would be a nearly 35% decrease for the scenario discussed above. For larger proteins, which allow a greater influx of water molecules, the decrease would be even more drastic (77). Such an interpretation of the NMRD data, although it is apparently consistent with the conclusions of the previously mentioned studies (13,56), appears counterintuitive when viewed in light of arguments put forward in a comprehensive review on protein conformational transitions, solvation, and the NMRD technique (77). To be specific, it has been pointed out that in most studies, the dimensions of globular proteins are estimated by measurement of their hydrodynamic radii (R_h), which have been shown to be significantly affected by energy dissipation due to friction (19). Since the MG state is more labile and has greater conformational flexibility, the discrepancy between its actual linear dimensions and the hydrodynamic radii is likely to be higher. However, compared to calorimetric, densitometric, dynamic light scattering, and sound absorption experiments, NMR studies report a greater compaction of the MG state (79–81). In one study, the experimentally obtained R_h was scaled to obtain the radius of gyration (79). High solvent influx consistent with a less compact model of the MG state may therefore not provide an accurate description of the true extent of hydration. Based on a more recent NMRD work, researchers reported that the rotational relaxation of the vast majority of surface waters hydrating a protein is slowed relative to bulk waters by a factor of ~2, whereas ρ_s ends up being between 4 and 5 due to the small number of very strongly associated water molecules (19). Hence, a dramatic decrease in ρ_s can only be brought about by the release of all strongly bound water molecules.

Our simulation of the subcompact ensemble shows only a marginal increase in the extent of solvent penetration. In contrast to earlier reports of a 55% increase in solvation of the molten globule state, we find a <9% increase due to solvent influx. The shift in energetics of the protein-solvent interactions in the partially denatured ensemble suggests that the change in solvation could contribute to decreased stability of the intermediate molten globule state. We show explicitly that the subcompact states have lower surface density of water compared to the native state. These changes are accompanied by a marginal but distinctive increase in mobility of the surface water dynamics. The ~12% downward shift in the mean rotational correlation time results in only a 15% decrease in ρ_s in the denatured ensemble, compared to the N state. This value is substantially less than the nearly 40% change that would have accompanied the high solvent influx predicted earlier. The reproduction of the constancy of the NMRD parameter $N_s\rho_s$ is the result of subtle changes in solvation number and dynamics between the native state and the partially denatured ensemble, and is consistent with the interpretation of NMRD data (77).

This study, based on the simulations of the native and partially denatured states of the HαLA protein, is an attempt to understand aspects of solvent dynamical behavior that accompany conformational changes of a protein along its folding landscape. It should be noted here that intrinsically unstructured proteins have been shown to bind much larger amounts of water than globular proteins (15). Such systems are highly disordered in their functional native form, and the dynamical properties of their hydration layer are likely to be different from that of partially unfolded globular proteins. Rather, the conclusions reached in this study ought to qualitatively represent phenomenological changes observed in the folding/unfolding of compact globular proteins. The values of the dynamic parameters and interaction energies, however, are likely to be dependent on the specific system under study (for example, $N_s\rho_s$ has different values for different globular proteins). Also, changes in the solvent environment, such as those brought about by the addition of salt, and by perturbations to the water-protein interactions and hydrogen-bonding network, can alter not only the dynamical parameters, but also the relative changes observed in one conformational state over another.

This work was supported by the National Science Foundation (Grants CHE-0417158 and CHE-0750175). We are grateful to Pinaki Sinha for assistance with data analysis.

REFERENCES

1. Gast, K., D. Zirwer, H. Welfle, V. E. Bychkova, and O. B. Ptitsyn. 1986. Quasielastic light scattering from human α-lactalbumin: comparison of molecular dimensions in native and ''molten globule'' states. *Int. J. Biol. Macromol.* 8:231–236.
2. Pal, S. K., J. Peon, B. Bagchi, and A. H. Zewail. 2002. Biological water: femtosecond dynamics of macromolecular hydration. *J. Phys. Chem. B.* 106:12376–12395.
3. Sen, P., S. Mukherjee, P. Dutta, A. Halder, D. Mandal, R. Banerjee, S. Roy, and K. Bhattacharyya. 2003. Solvation dynamics in the molten globule state of a protein. *J. Phys. Chem. B.* 107:14563–14568.
4. Samaddar, S., A. K. Mandal, S. K. Mondal, K. Sahu, K. Bhattacharyya, and S. Roy. 2006. Solvation dynamics of a protein in the pre molten globule state. *J. Phys. Chem. B.* 110:21210–21215.
5. Zhang, L., L. Wang, Y.-T. Kao, W. Qiu, Y. Yang, O. Okobiah, and D. Zhong. 2007. Mapping hydration dynamics around a protein surface. *Proc. Natl. Acad. Sci. USA.* 104:18461–18466.
6. Ferrand, M., A. J. Dianoux, W. Petry, and G. Zaccai. 1993. Thermal motions and function of bacteriorhodopsin in purple membranes: effects of temperature and hydration studied by neutron scattering. *Proc. Natl. Acad. Sci. USA.* 90:9668–9672.
7. Svergun, D. I., S. Richard, M. H. J. Koch, Z. Sayers, S. Kuprin, and G. Zaccai. 1998. Protein hydration in solution: experimental observation by x-ray and neutron scattering. *Proc. Natl. Acad. Sci. USA.* 95:2267–2272.
8. Teeter, M. M., A. Yamano, B. Stec, and U. Mohanty. 2001. On the nature of a glassy state of matter in a hydrated protein: relation to protein function. *Proc. Natl. Acad. Sci. USA.* 98:11242–11247.
9. Doster, W., and M. Settles. 2005. Protein-water displacement distributions. *Biochim. Biophys. Acta.* 1749:173–186.
10. Wood, K., M. Plazanet, F. Gabel, B. Kessler, D. Oesterhelt, D. J. Tobias, G. Zaccai, and M. Weik. 2007. Coupling of protein and hydration-water dynamics in biological membranes. *Proc. Natl. Acad. Sci. USA.* 104:18049–18054.
11. Wood, K., A. Frolich, A. Paciaroni, M. Moulin, M. Hartlein, G. Zaccai, D. J. Tobias, and M. Weik. 2008. Coincidence of dynamical transitions in a soluble protein and its hydration water: direct measurements by neutron scattering and MD simulations. *J. Am. Chem. Soc.* 130:4586–4587.
12. Stanley, C., S. Krueger, V. A. Parsegian, and D. C. Rau. 2008. Protein structure and hydration probed by SANS and osmotic stress. *Biophys. J.* 94:2777–2789.
13. Kutyshenko, V. P., and M. Cortijo. 2000. Water-protein interactions in the molten-globule state of carbonic anhydrase b: an NMR spin-diffusion study. *Protein Sci.* 9:1540–1547.
14. Krzystyniak, M., G. Shen, J. H. Golbeck, and M. L. Antonkine. 2008. Investigation of water bound to photosystem I with multiquantum filtered 17O nuclear magnetic resonance. *J. Chem. Phys.* 128:014503–014515.
15. Bokor, M., V. Csizmok, D. Kovacs, P. Banki, P. Friedrich, P. Tompa, and K. Tompa. 2005. NMR relaxation studies on the hydrate layer of intrinsically unstructured proteins. *Biophys. J.* 88:2030–2037.
16. Denisov, V. P., and B. Halle. 1995. Protein hydration dynamics in aqueous solution: a comparison of bovine pancreatic trypsin inhibitor and ubiquitin by oxygen-17 spin relaxation dispersion. *J. Mol. Biol.* 245:682–697.
17. Denisov, V. P., and B. Halle. 1996. Protein hydration dynamics in aqueous solution. *Faraday Disc.* 103:227–244.
18. Denisov, V. P., B. H. Jonsson, and B. Halle. 1999. Hydration of denatured and molten globule proteins. *Nat. Struct. Biol.* 6:253–260.
19. Halle, B., and M. Davidovic. 2003. Biomolecular hydration: from water dynamics to hydrodynamics. *Proc. Natl. Acad. Sci. USA.* 100: 12135–12140.
20. Modig, K., E. Liepinsh, G. Otting, and B. Halle. 2004. Dynamics of protein and peptide hydration. *J. Am. Chem. Soc.* 126:102–114.
21. Giuffrida, S., G. Cottone, and L. Cordone. 2006. Role of solvent on protein-matrix coupling in MbCO embedded in water-saccharide systems: a Fourier transform infrared spectroscopy study. *Biophys. J.* 91:968–980.
22. Knab, J., J.-Y. Chen, and A. Markelz. 2006. Hydration dependence of conformational dielectric relaxation of lysozyme. *Biophys. J.* 90:2576–2581.
23. Xu, J., K. W. Plaxco, and S. J. Allen. 2006. Probing the collective vibrational dynamics of a protein in liquid water by terahertz absorption spectroscopy. *Protein Sci.* 15:1175–1181.
24. Ebbinghaus, S., S. J. Kim, M. Heyden, X. Yu, U. Heugen, M. Gruebele, D. M. Leitner, and M. Havenith. 2007. An extended dynamical hydration shell around proteins. *Proc. Natl. Acad. Sci. USA.* 104: 20749–20752.
25. Ebbinghaus, S., S. J. Kim, M. Heyden, X. Yu, M. Gruebele, D. M. Leitner, and M. Havenith. 2008. Protein sequence- and pH-dependent hydration probed by terahertz spectroscopy. *J. Am. Chem. Soc.* 130: 2374–2375.
26. Lounnas, V., and B. M. Pettitt. 1994. Distribution function implied dynamics versus residence times and correlations: solvation shells of myoglobin. *Proteins.* 18:148–160.
27. Rocchi, C., A. R. Bizzarri, and S. Cannistraro. 1998. Water dynamical anomalies evidenced by molecular-dynamics simulations at the solvent-protein interface. *Phys. Rev. E.* 57:3315–3325.
28. Marchi, M., F. Sterpone, and M. Ceccarelli. 2002. Water rotational relaxation and diffusion in hydrated lysozyme. *J. Am. Chem. Soc.* 124:6787–6791.
29. Tarek, M., and D. J. Tobias. 1999. Environmental dependence of the dynamics of protein hydration water. *J. Am. Chem. Soc.* 121:9740–9741.
30. Pizzitutti, F., M. Marchi, F. Sterpone, and P. J. Rossky. 2007. How protein surfaces induce anomalous dynamics of hydration water. *J. Phys. Chem. B.* 111:7584–7590.
31. Rhee, Y. M., E. J. Sorin, G. Jayachandran, E. Lindahl, and V. S. Pande. 2004. Simulations of the role of water in the protein-folding mechanism. *Proc. Natl. Acad. Sci. USA.* 101:6456–6461.
32. Barth, P., T. Alber, and P. B. Harbury. 2007. Accurate, conformation-dependent predictions of solvent effects on protein ionization constants. *Proc. Natl. Acad. Sci. USA.* 104:4898–4903.
33. Vitkup, D., D. Ringel, G. A. Petsko, and M. Karplus. 2000. Solvent mobility and the protein ''glass'' transition. *Nat. Struct. Biol.* 7:34–38.
34. Tarek, M., G. J. Martyna, and D. J. Tobias. 2000. Amplitudes and frequencies of protein dynamics: analysis of discrepancies between neutron scattering and molecular dynamics simulations. *J. Am. Chem. Soc.* 122:10450–10451.
35. Heberle, J., J. Fitter, H. J. Sass, and G. Büldt. 2000. Bacteriorhodopsin: the functional details of a molecular machine are being resolved. *Biophys. Chem.* 85:229–248.
36. Mattos, C. 2002. Protein-water interactions in a dynamic world. *Trends Biochem. Sci.* 27:203–208.
37. Papoian, G. A., J. Ulander, M. P. Eastwood, Z. Luthey-Schulten, and P. G. Wolynes. 2004. Water in protein structure prediction. *Proc. Natl. Acad. Sci. USA.* 101:3352–3357.
38. Daggett, V. 2006. Protein folding-simulation. *Chem. Rev.* 106:1898–1916.
39. Levy, Y., and J. N. Onuchic. 2006. Water mediation in protein folding and molecular recognition. *Annu. Rev. Biophys. Biomol. Struct.* 35: 389–415.
40. Cheung, M. S., A. E. Garcia, and J. N. Onuchic. 2002. Protein folding mediated by solvation: water expulsion and formation of the hydrophobic core occur after the structural collapse. *Proc. Natl. Acad. Sci. USA.* 99:685–690.
41. Harano, Y., and M. Kinoshita. 2004. Large gain in translational entropy of water is a major driving force in protein folding. *Chem. Phys. Lett.* 399:342–348.

42. Jas, G. S., W. A. Eaton, and J. Hofrichter. 2001. Effect of viscosity on the kinetics of α-helix and β-hairpin formation. *J. Phys. Chem. B.* 105: 261–272.
43. Pradeep, L., and J. B. Udgaonkar. 2007. Diffusional barrier in the unfolding of a small protein. *J. Mol. Biol.* 366:1016–1028.
44. Dyson, H. J., and P. E. Wright. 1998. Equilibrium NMR studies of unfolded and partially folded proteins. *Nat. Struct. Mol. Biol.* 5: 499–503.
45. Cheung, M. S., L. L. Chavez, and J. N. Onuchic. 2004. The energy landscape for protein folding and possible connections to function. *Polymer.* 45:547–555.
46. Bandyopadhyay, S., S. Chakraborty, and B. Bagchi. 2006. Exploration of the secondary structure specific differential solvation dynamics between the native and molten globule states of the protein HP-36. *J. Phys. Chem. B.* 110:20629–20634.
47. Chakraborty, S., and S. Bandyopadhyay. 2008. Dynamics of water in the hydration layer of a partially unfolded structure of the protein HP-36. *J. Phys. Chem. B.* 112:6500–6507.
48. Kuwajima, K. 1989. The molten globule state as a clue for understanding the folding and cooperativity of globular-protein structure. *Proteins.* 6:87–103.
49. Ptitsyn, O. B. 1995. Molten globule and protein folding. *Adv. Protein Chem.* 47:83–229.
50. Wolynes, P. G., J. N. Onuchic, and D. Thirumalai. 1995. Navigating the folding routes. *Science.* 267:1619–1620.
51. Sutovsky, H., and E. Gazit. 2004. The von Hippel-Lindau tumor suppressor protein is a molten globule under native conditions: implications for its physiological activities. *J. Biol. Chem.* 279:17190–17196.
52. Mahley, R. W., and Y. Huang. 2006. Apolipoprotein (apo) E4 and Alzheimer's disease: unique conformational and biophysical properties of apoE4 can modulate neuropathology. *Acta. Neurolog. Scand.* 114: 8–14.
53. Tarek, M., and D. J. Tobias. 2000. The dynamics of protein hydration water: a quantitative comparison of molecular dynamics simulations and neutron-scattering experiments. *Biophys. J.* 79:3244–3257.
54. Abseher, R., H. Schreiber, and O. Steinhauser. 1996. The influence of a protein on water dynamics in its vicinity investigated by molecular dynamics simulation. *Proteins.* 25:366–378.
55. Settles, M., and W. Doster. 1996. Anomalous diffusion of adsorbed water: a neutron scattering study of hydrated myoglobin. *Faraday Disc.* 103:269–279.
56. Kharakoz, D. P., and V. E. Bychkova. 1997. Molten globule of human α-lactalbumin: hydration, density, and compressibility of the interior. *Biochemistry.* 36:1882–1890.
57. Fink, A. L. 1995. Compact intermediate states in protein folding. *Annu. Rev. Biophys. Biomol. Struct.* 24:495–522.
58. Paci, E., L. J. Smith, C. M. Dobson, and M. Karplus. 2001. Exploration of partially unfolded states of human α-lactalbumin by molecular dynamics simulation. *J. Mol. Biol.* 306:329–347.
59. Acharya, K. R., J. Ren, D. I. Stuart, D. C. Phillips, and R. E. Fenna. 1991. Crystal structure of human α-lactalbumin at 1.7 Å resolution. *J. Mol. Biol.* 221:571–581.
60. Qiu, D., P. S. Shenkin, F. P. Hollinger, and W. C. Still. 1997. The GB/SA continuum model for solvation. A fast analytical method for the calculation of approximate Born radii. *J. Phys. Chem. A.* 101:3005–3014.
61. Kuwajima, K., Y. Hiraoka, M. Ikeguchi, and S. Sugai. 1985. Comparison of the transient folding intermediates in lysozyme and α-lactalbumin. *Biochemistry.* 24:874–881.
62. Berendsen, H. J. C., J. R. Grigera, and T. P. Straatsma. 1987. The missing term in effective pair potentials. *J. Phys. Chem.* 91:6269–6271.
63. Kale, L., R. Skeel, M. Bhandarkar, R. Brunner, A. Gursoy, N. Krawetz, J. Phillips, A. Shinozaki, K. Varadarajan, and K. Schulten. 1999. NAMD2: greater scalability for parallel molecular dynamics. *J. Comput. Phys.* 151:283–312.
64. Brooks B. R., R. E. Bruccoleri, B. D. Olafson, D. J. States, S. Swaminathan, and M. Karplus. 1983. CHARMM: a program for macromolecular energy, minimization, and dynamics calculations. *J. Comput. Chem.* 4:187–217.
65. Martyna, G. J., D. J. Tobias, and M. L. Klein. 1994. Constant pressure molecular dynamics algorithms. *J. Chem. Phys.* 101:4177–4189.
66. Feller S. E., Y. Zhang, R. W. Pastor, and B. R. Brooks. 1995. Constant pressure molecular dynamics simulation: the Langevin piston method. *J. Chem. Phys.* 103:4613–4621.
67. Martyna, G. J., M. E. Tuckerman, D. J. Tobias, and M. L. Klein. 1996. Explicit reversible integrators for extended systems dynamics. *Mol. Phys.* 87:1117–1157.
68. Essmann, U., L. Perera, M. L. Berkowitz, T. Darden, H. Lee, and L. G. Pedersen. 1995. A smooth particle mesh Ewald method. *J. Chem. Phys.* 103:8577–8593.
69. Humphrey, W., A. Dalke, and K. Schulten. 1996. VMD: visual molecular dynamics. *J. Mol. Graph.* 14:33–38.
70. Halle, B., and H. Wennerstroem. 1981. Nearly exponential quadrupolar relaxation. A perturbation treatment. *J. Magn. Reson.* 44:89–100.
71. Denisov, V. P., K. Venu, J. Peters, H. D. Horlein, and B. Halle. 1997. Orientational disorder and entropy of water in protein cavities. *J. Phys. Chem. B.* 101:9380–9389.
72. Denisov, V. P., G. Carlstrom, K. Venu, and B. Halle. 1997. Kinetics of DNA hydration. *J. Mol. Biol.* 268:118–136.
73. Denisov, V. P., J. L. Schlessman, B. E. Garcia-Moreno, and B. Halle. 2004. Stabilization of internal charges in a protein: water penetration or conformational change? *Biophys. J.* 87:3982–3994.
74. Burling, F. T., W. I. Weis, K. M. Flaherty, and A. T. Brunger. 1996. Direct observation of protein solvation and discrete disorder with experimental crystallographic phases. *Science.* 271:72–77.
75. Merzel, F., and J. C. Smith. 2002. Is the first hydration shell of lysozyme of higher density than bulk water? *Proc. Natl. Acad. Sci. USA.* 99:5378–5383.
76. Makarov, V., B. M. Pettitt, and M. Feig. 2002. Solvation and hydration of proteins and nucleic acids: a theoretical view of simulation and experiment. *Acc. Chem. Res.* 35:376–384.
77. Halle, B., V. P. Denisov, K. Modig, and M. Davidoc. 2005. Protein conformational transitions as seen from the solvent: magnetic relaxation dispersion studies of water, co-solvent, and denaturant interactions with nonnative proteins. *In* Protein Folding Handbook. J. Buchner and T. Kiefhaber, editors. Wiley-VCH, Weinheim, Germany. 201–242.
78. Shortle, D. 1999. Protein folding as seen from water's perspective. *Nat. Struct. Biol.* 6:203–205.
79. Redfield, C., B. A. Schulman, M. A. Milhollen, P. S. Kim, and C. M. Dobson. 1999. α-Lactalbumin forms a compact molten globule in the absence of disulfide bonds. *Nat. Struct. Biol.* 6:948–952.
80. Balbach, J. 2000. Compaction during protein folding studied by real-time NMR diffusion experiments. *J. Am. Chem. Soc.* 122:5887–5888.
81. Chakraborty, S., V. Ittah, P. Bai, L. Luo, E. Haas, and Z. Y. Peng. 2001. Structure and dynamics of the α-lactalbumin molten globule: fluorescence studies using proteins containing a single tryptophan residue. *Biochemistry.* 40:7228–7238.